Unimolecular Reactions of Protonated Hydrogen Peroxide: A Quantum Chemical Survey

Elisabeth Leere Øiestad,[†] Jeremy N. Harvey,[‡] and Einar Uggerud*[,†]

Department of Chemistry, University of Oslo, P. O. Box 1033 Blindern, N-0315 Oslo, Norway, and School of Chemistry, University of Bristol, Cantock's Close, Bristol BS8 1TS, United Kingdom

Received: February 7, 2000; In Final Form: April 25, 2000

The unimolecular chemistry of the system $[HOOH]H^+$ has been investigated using ab initio quantum chemical methods. In analogy with the isoelectronic systems—$[H_2NNH_2]H^+$ and $[HONH_2]H^+$, in this paper subject to more detailed studies than previously—the lowest energy pathway for decomposition of protonated hydrogen peroxide is loss of an oxygen atom in its triplet electronic state, giving H_3O^+ as the ionic product. This process requires a crossover from the singlet to the triplet potential energy surface, and the minimum energy crossing point was located. The proton affinity was also calculated and found to be in good accordance with one experimental determination.

Introduction

Hydrogen peroxide, H_2O_2, is a powerful, and yet environmental friendly, oxidizing agent, since it forms only water and oxygen upon decomposition.[1] For this reason it has replaced chlorine oxides for bleaching in the pulp and paper industry.[2] Hydrogen peroxide is unstable in both acidic and basic solution and in the presence of transition metals.[3] The correspondence between the decomposition chemistry of H_2O_2 and its action as an oxidant is quite obvious. As an example we will mention Fenton's reagent, which is made by reaction between Fe^{2+} and H_2O_2. This Fe/H_2O_2 system is also highly relevant in connection with biological oxidation,[4−6] as in the cytochrome enzymes.[7−9]

Even in the absence of a transition metal, hydrogen peroxide can be activated. In superacidic solutions, protonated hydrogen peroxide demonstrates extraordinary oxidative behavior, by specifically inserting an oxygen into aliphatic and aromatic C−H bonds, giving aldehydes/ketones or alcohols, respectively.[10,11] Although the solution chemistry of protonated hydrogen peroxide has received some attention—also theoretically,[12] little is known about its gas-phase behavior.

Only one experimental report appears to exist on the gas-phase chemistry of $[HOOH]H^+$, namely, a flowing afterglow study by Lindinger et al.[13] They were able to observe proton transfer to and from H_2O_2, making a prediction of the proton affinity of $PA = 675 \pm 45$ kJ mol^{-1}.

In this article we present results from a theoretical study of the unimolecular gas-phase chemistry of protonated hydrogen peroxide. To our knowledge, this is the first detailed investigation of this type.

Theoretical Methods

Quantum chemical calculations were carried out using the program system GAUSSIAN 98.[14] The 6-31G(d,p) basis set was employed.[15]

All relevant critical points (reactants, transition structures, intermediates, and products) of the potential energy surface were characterized by complete optimization of the molecular geometries (MP2/6-31G(d,p)). Harmonic frequencies were obtained by diagonalizing the mass-weighted Cartesian force constant matrix, calculated from the analytical second derivatives of the total energy (the Hessian). Harmonic frequencies obtained in this manner were used to calculate the zero point vibrational energies (zpve). Total energies were calculated by including the MP2/6-31G(d,p) zero point vibrational energies scaled by a factor of 0.9608.[16] The correct connection between each of the transition structures (having one negative eigenvalue of the Hessian) and the corresponding minima was verified by calculating the intrinsic reaction coordinate.[17]

To locate minimum energy crossing points between the singlet and triplet potential energy surfaces, the MECP approach was used.[18]

To calculate the spin−orbit coupling at the minimum energy crossing point, designated **CP1** (see below), the approximate one-electron operator method[19] as implemented in the December 1998 version of the Gamess-USA program[20] was used. Individually optimized CASSCF(2,2) wave functions together with a DZP basis set were used to describe the singlet and triplet states. The H_{SOC} reported is the root mean square (rms) value of the coupling of the singlet and the three triplet components.

To obtain accurate proton affinities, calculations using the G2(MP2) scheme[21−23] were performed for some selected molecules.

Results and Discussion

Protonation of H_2O_2 and Proton Affinity. The absolute potential energy minimum of the molecular system corresponds to the protonated hydrogen peroxide molecule, $^1HOOH_2^+$ (**1**), in its singlet spin state (Figure 1, Table 1). Comparison between the molecular geometries of $HOOH_2^+$ (**1**) and its corresponding base, HOOH (**2**), shows that the O−O distance is shortened by 0.007 Å upon protonation (Figure 2). There exists one previous accurate computational study of hydrogen peroxide and its

* To whom correspondence should be addressed. E-mail: einar.uggerud@kjemi.uio.no.
[†] University of Oslo.
[‡] University of Bristol.

10.1021/jp000480g CCC: $19.00
Published on Web 08/19/2000

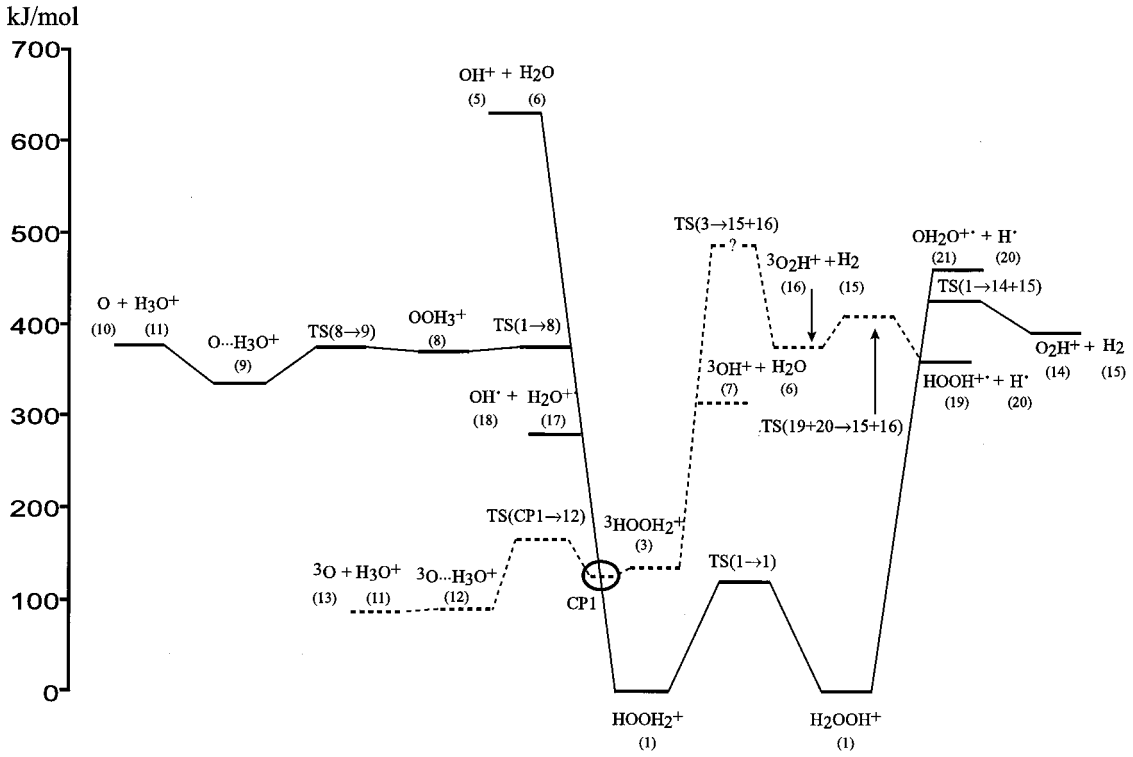

Figure 1. Potential energy diagram for the $[HOOH]H^+$ system from the MP2/6-31G(d,p) calculations. Relative energies indicated are in kilojoules per mole and include zpve corrections.

protonated form,[24] and the data published in that study confirm our observation of similar O−O bond lengths. In addition, the O−O stretching frequency is practically the same for $HOOH_2^+$ and HOOH. Our results also show that in hydrazine the N−N bond distance increases from 1.437 to 1.445 Å, while in hydroxylamine the N−O bond is 1.451 Å compared to 1.409 Å in the N-protonated and 1.479 Å in the O-protonated forms. This behavior is quite unexpected. Most organic molecules display significant elongation of bonds connecting the atom which is protonated to its next neighbors.[25]

We want to be careful in providing speculative explanations of the observed bond shortenings upon protonation. Some rehybridization is obviously in operation, either by strengthening the bonding or weakening the antibonding O−O interaction. Experimental and computational evidence has shown that the O−O bonds of halogen peroxides are shorter than in hydrogen peroxide.[26] For example, the O−O bond in F−O−O−F is only 1.22 Å; making it as short as the double bond in dioxygen. This may be attributed to the σ-attracting and π-donating properties of the halogens. The same phenomenon is also a likely cause of the so-called α effect, used to explain the enhanced reactivity of HO_2^- and similar nucleophiles.[27−29]

A transition structure, **TS(1→1)**, only 119 kJ mol^{-1} above protonated hydrogen peroxide allows for degenerate proton transfer from one oxygen to the other.

The proton affinity of HOOH was calculated using the G2-(MP2) scheme to be $PA_{calc}[HOOH] = 668$ kJ mol^{-1}. This value is in good agreement with the experimental value[13,30] which is $PA_{exp}[HOOH] \approx 675$ kJ mol^{-1}, and one previous ab initio value.[13,30] We have previously studied protonation of two closely related species, hydrazine and hydroxylamine, and the unimolecular chemistry of their protonated forms. It was interesting to see how the proton affinities of these species and hydrogen peroxide are related. Two stable isomers of protonated hydroxylamine exist, depending on whether protonation occurs on the oxygen or the nitrogen. Very interestingly simple data analysis shows that the average of the O- and N-proton affinities is very close to the average in proton affinities of hydrogen peroxide and hydrazine (Table 2):

$$PA[HONH_2] + PA[HONH_2] = PA[HOOH] + PA[H_2NNH_2] \quad (1)$$

The triplet form of protonated hydrogen peroxide, $^3HOOH_2^+$ (**3**), lies 133 kJ mol^{-1} above the singlet. This energy difference is smaller than for the corresponding bases, ^{3}HOOH (**4**) and ^{1}HOOH (**2**), that differ by 204 kJ mol^{-1} (Table 1).

Unimolecular Water Loss. Previous experimental and computational experience with protonated hydrazine[31] and protonated hydroxylamine[32] has taught us that it is imperative to include the triplet potential energy surface when considering the unimolecular chemistry. This is related to the fact that both O and NH are triplets in their ground states.[33] It is now well-established that even for molecules containing only first and second row elements, spin−orbit coupling may lead to effective nonadiabatic coupling between potential energy surfaces of different electron spin.[18,34−39]

Direct O−O heterolytic bond dissociation of protonated hydrogen peroxide gives the hydroxyl cation and water. On the singlet surface this reaction

$$^1HOOH_2^+ \ (\mathbf{1}) \rightarrow {}^1OH^+ \ (\mathbf{5}) + H_2O \ (\mathbf{6}) \quad (2)$$

is very unfavorable (Figure 1), by having $\Delta E^\circ = 629$ kJ mol^{-1}. On the other hand, far more stable products are formed on the triplet surface:

$$^3HOOH_2^+ \ (\mathbf{1}) \rightarrow {}^3OH^+ \ (\mathbf{7}) + H_2O \ (\mathbf{6}) \quad (3)$$

This reaction is endoergic by only $\Delta E^\circ = 180$ kJ mol^{-1} (relative to triplet protonated hydrogen peroxide). Neither reaction 2 nor reaction 3 has a reverse barrier.

TABLE 1: Energies from ab Initio Quantum Chemical Calculations

structure	MP2/6-31(d,p) electronic energy, hartrees	E_{zpv},[a] kJ/mol
OH_2OH^+ (**1**)	−151.424 31	101.3
OHOH (**2**)	−151.152 04	67.2
$^3OH_2OH^+$ (**3**)	−151.371 36	95.4
^{3}OHOH (**4**)	−151.070 69	58.0
OH^+ (**5**)	−74.954 64	18.7
H_2O (**6**)	−76.219 79	55.2
$^3OH^+$ (**7**)	−75.074 76	18.7
OOH_3^+ (**8**)	−151.280 66	93.5
$O\cdots H_3O^+$ (**9**)	−151.293 32	92.0
O (**10**)	−74.769 95	
H_3O^+ (**11**)	−76.506 11	89.0
$^3O\cdots H_3O^+$ (**12**)	−151.386 22	90.3
^{3}O (**13**)	−74.880 04	
O_2H^+ (**14**)	−150.103 06	34.9
H_2 (**15**)	−1.157 66	26.5
$^3O_2H^+$ (**16**)	−150.108 56	34.0
$H_2O^{\bullet+}$ (**17**)	−75.774 24	48.8
$OH^\bullet$ (**18**)	−75.532 09	22.1
$HOOH^{\bullet+}$ (**19**)	−150.784 60	88.0
$H^\bullet$ (**20**)	−0.498 23	
$OH_2O^{\bullet+}$ (**21**)	−150.738 31	67.2
$NH_2NH_3^+$ (**22**)	−111.888 43	176.1
^{3}NH (**23**)	−55.067 94	19.6
NH_4^+ (**24**)	−56.733 68	128.4
$NH_2OH_2^+$ (**25**)	−131.685 47	140.9
NH_3OH^+ (**26**)	−131.642 15	136.2
$^3NH_2OH_2^+$ (**27**)	−131.586 13	120.3
$^3NH_3OH^+$ (**28**)	−131.583 38	115.1
CP1	−151.369 88	85.5
CP2	−111.784 49	148.2
CP3	−151.577 73	116.7
CP4	−151.582 16	114.5
TS(1→1)	−151.373 31	86.4
TS(1→8)	−151.277 53	86.5
TS(8→9)	−151.276 10	72.6
TS(1→14+15)	−151.251 51	89.9
TS(CP1→12)	−151.355 01	83.1
TS(19+20→15+16)	−151.253 99	65.5
TS(25→26)	−151.598 09	122.2
TS(27→28)	−151.546 18	110.9
TS(CP3→11+23)	−151.576 12	114.5
TS(CP4→13+24)	−151.551 07	117.4

[a] $0.9608E_{zpv}$(MP2/6-31(d,p)).

Unimolecular O Loss. Heterolytic bond dissociation may also lead to an alternative, more stable set of products: the higher proton affinity of water compared to the oxygen atom (irrespective of spin state) makes the proton-transfer products thermochemically more favorable:

$$HOOH_2^+ \rightarrow O + H_3O^+ \qquad (4)$$

In agreement with very precise thermochemical data,[33] the triplet/singlet separation increases slightly upon protonation of O. On the singlet surface the above reaction is rather energy demanding, being endoergic by $\Delta E° = 327$ kJ mol^{-1}, while on the triplet surface (relative to $^3HOOH_2^+$) it is exoergic by $\Delta E° = -45$ kJ mol^{-1}!

On the singlet surface, a rearrangement process leading to the products of eq 4 seems to be the most feasible. The first step is rearrangement of $^1HOOH_2^+$ (**1**) into the transient species $^1OOH_3^+$ (**8**). We do realize that the flatness of the potential energy surface in this region makes it questionable whether OOH_3^+ really is an intermediate, despite the fact that the MP2/6-31G(d,p) calculation shows it to be a shallow minimum. In any case, this is probably not an issue of great concern for the actual dynamics of the process. From this isomer the reaction path leads to the hydrogen bonded ion/neutral complex $^1O\cdots H_3O^+$ (**9**), which ultimately decomposes to give products. The calculations indicate that the point of highest potential energy for the overall process is the separated products at 377 kJ mol^{-1}. In summary the mechanism is

$$^1HOOH_2^+ (\mathbf{1}) \rightarrow {}^1OOH_3^+ (\mathbf{8}) \rightarrow {}^1O\cdots H_3O^+ (\mathbf{9}) \rightarrow {}^1O (\mathbf{10}) + H_3O^+ (\mathbf{11}) \qquad (5)$$

As already pointed out, it is probably not realistic to consider formation of the corresponding products $^3O + H_3O^+$ directly from triplet protonated hydrogen peroxide. When we instead, in close analogy with the previously studied systems $[H_2NNH_2]$-H^+ and $[HONH_2]H^+$,[31,32] consider the possibility of a crossover from the singlet to the triplet surface, we find the highly interesting mechanism

$$^1HOOH_2^+ (\mathbf{1}) \rightarrow {}^3O\cdots H_3O^+ (\mathbf{12}) \rightarrow {}^3O (\mathbf{13}) + H_3O^+ (\mathbf{11}) \qquad (6)$$

Explicit calculation of the reaction route, using the MECP method previously described, locates the minimum energy crossing point—**CP1**—at the geometry shown in Figure 2. Intramolecular proton transfer then gives $^3O\cdots H_3O^+$ (**12**), which upon decomposition leads to the final products. The transition structure, TS(**CP1** → **12**), is the highest point of this reaction mechanism at 164 kJ mol^{-1} relative to $^1HOOH_2^+$ (**1**). On the basis of the existing computational evidence (Figure 1), we see that it represents the minimum energy pathway for unimolecular decomposition of protonated hydrogen peroxide.

Using an approximate method (see Theoretical Methods), the spin−orbit coupling matrix element between singlet and triplet wave functions at **CP1** was calculated as $H_{SOC} = 57$ cm^{-1}. On the basis of this value and our previous experience with similar systems, see above, we are confident that this coupling is sufficient to induce rather efficient surface crossing at **CP1** for systems having an energy close to that of TS(**CP1** → **12**). A similar argument will also hold for **CP2**−**CP4**; see below.

While not quantitatively accurate, the MP2/6-31G(d,p) approach used in this study is of sufficient accuracy to characterize the reaction mechanism. To explicitly check that the relative energy of the key **CP1** is obtained correctly at this level of theory, further calculations have been performed at a variety of other, higher levels. In all cases, the relative electronic energy of the $^1HOOH_2^+$ (**1**), CP1, and ^3O (**13**) + H_3O^+ (**11**) points was found to be essentially the same as with MP2/6-31G(d,p). For instance, with CCSD(T)/cc-pVTZ//MP2/6-311G(d,p) (where **CP1** was optimized using the hybrid method of ref 18), these points lie respectively at 0.0, 158.2, and 114.4 kJ mol^{-1}, very close to the MP2/6-31G(d,p) electronic relative energies of 0.0, 142.9, and 100.2 kJ mol^{-1}. Because of the good agreement, these more computationally demanding calculations have not been pursued.

Although the electronic energy—as expected—is higher for **CP1** than for $^3HOOH_2^+$ (**3**), inclusion of zero point vibrational energy corrections, as in Figure 1, leads to **CP1** apparently becoming lower in energy than **3**. This is due to the approximate nature of the zero-point energy correction based on harmonic potentials, which is especially unreliable for crossing points such as **CP1**.

Unimolecular H_2 Loss. Loss of dihydrogen, a reaction observed for many similar molecules,[40] seems to be rather

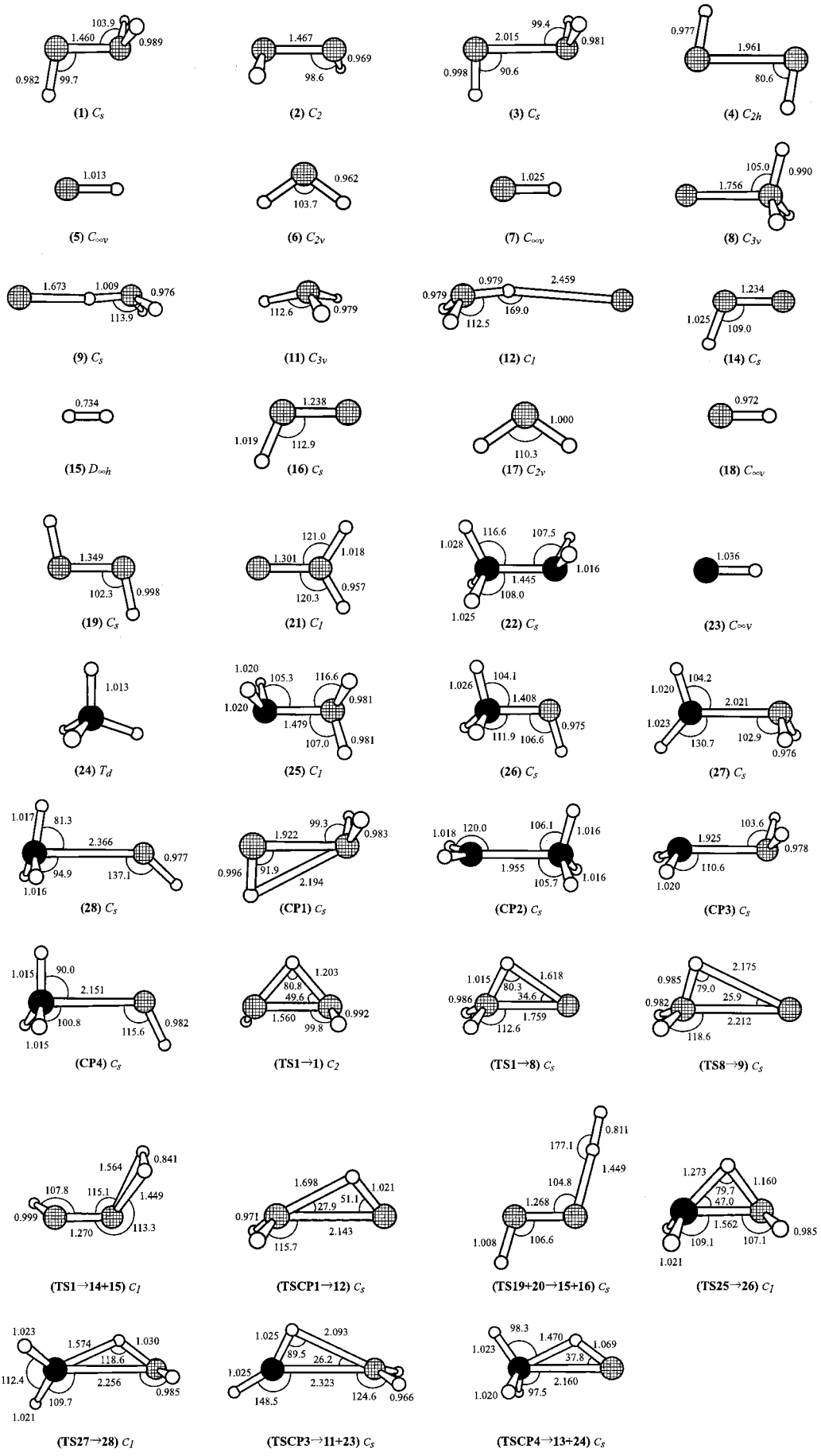

Figure 2. Structures of the stationary points obtained with MP2/6-31G(d,p). Bond distances indicated are in angstrom units. The Cartesian coordinates for the structures referred to in this paper may be obtained from the authors upon request.

TABLE 2: Thermochemical Data[a]

molecule	H(G2MP2)
H_2NNH_2	−111.673 444
$H_2NNH_3^+$	−112.000 555
$HONH_2$	−131.525 469
$HONH_3^+$	−131.834 206
$^+H_2ONH_2$	−131.793 185
HOOH	−151.357 144
$HOOH_2^+$	−151.609 135

[a] Absolute enthalpy at 298 K (electronic and nuclear potential energy including zero-point vibrational energy and thermal contributions, plus enthalpy's volume part) calculated with G2(MP2), in hartrees.

unfavorable for hydrogen peroxide:

$$^1HOOH_2^+ \textbf{(1)} \rightarrow {}^1O_2H^+ \textbf{(14)} + H_2 \textbf{(15)} \quad (7)$$

$$^3HOOH_2^+ \textbf{(3)} \rightarrow {}^3O_2H^+ \textbf{(16)} + H_2 \textbf{(15)} \quad (8)$$

The calculations indicate that this process is endoergic by $\Delta E° = 390$ kJ mol^{-1} for the singlet, while the triplet products are 16 kJ mol^{-1} lower in potential energy (Figure 1). A transition structure for reaction 7, **TS(1→14+15)**, was located. With respect to the reactant it is "late" (product-like), which is reflected in the rather small barrier for the reverse reaction of $E_b = 35$ kJ mol^{-1}. The reaction corresponds to a 1,1-elimination. Despite considerable computational effort, we have so far not been able to locate the anticipated transition structure for reaction 8, **TS(3→16+15)** on the triplet surface.

Unimolecular OH Loss. Homolytic cleavage of the O−O bond gives the water radical cation and the hydroxyl radical

$$HOOH_2^+ \rightarrow H_2O^{\bullet +} \textbf{(17)} + OH^{\bullet} \textbf{(18)} \quad (9)$$

This is a direct bond cleavage, and it proceeds without the need to cross a barrier (zero reverse critical energy). The reaction endoergicity amounts to $\Delta E° = 279$ kJ mol^{-1}—so on the singlet surface it turns out to be a more likely reaction than the corresponding heterolytic bond dissociation. The quartet states of $H_2O^{\bullet +}$ and $OH^{\bullet}$ were not taken into accountin our calculations, as they are highly unstable molecular species.

Unimolecular H Loss. Loss of a hydrogen radical gives one of two $(O_2,H_2)^{\bullet +}$ isomers depending on which of the O−H bonds is cleaved.

$$HOOH_2^+ \rightarrow HOOH^{\bullet +} \textbf{(19)} + H^{\bullet} \textbf{(20)} \quad (10)$$

$$HOOH_2^+ \rightarrow OOH_2^{\bullet +} \textbf{(21)} + H^{\bullet} \textbf{(20)} \quad (11)$$

Of these the former reaction demands less energy with $\Delta E° = 358$ kJ mol^{-1}, while the latter has $\Delta E° = 459$ kJ mol^{-1}. Neither of these reactions has a barrier for the reverse reaction.

MECPs for $[H_2NNH_2]H^+$ and $[HONH_2]H^+$. The previous studies of protonated hydrazine and protonated hydroxylamine are incomplete in the sense that precise minimum energy crossing points of the singlet and triplet states were not determined. We are now in the position to present data on this.

The MP2/6-31G(d,p) potential energy surface of $(N_2,H_5)^+$ was given in Figures 2 and 5 of the $[H_2NNH_2]H^+$ paper.[31] As shown in that paper a singlet to triplet crossing on the route

$$^1NH_2NH_3^+ \textbf{(22)} \rightarrow {}^3NH \textbf{(23)} + NH_4^+ \textbf{(24)} \quad (12)$$

exists. The present calculation shows that the MECP, **CP2**, has the geometry displayed in Figure 2. The potential energy relative to **22** is 245 kJ mol^{-1}.

In the case of protonated hydroxylamine we observed NH loss which could be attributed to the reaction

$$^1NH_2OH_2^+ \textbf{(25)} \rightarrow {}^3NH \textbf{(23)} + H_3O^+ \textbf{(11)} \quad (13)$$

We have now located a minimum energy crossing point, **CP3**. This is illustrated in Figures 2 (structure) and 3 (energy

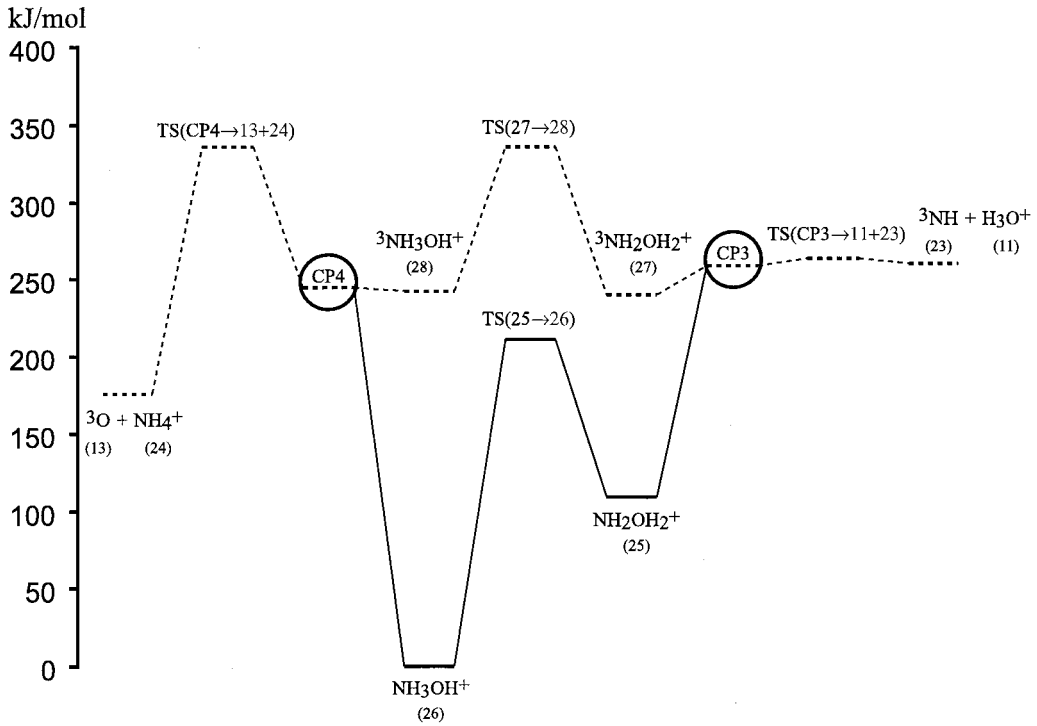

Figure 3. Potential energy diagram for the $[HONH_2]H^+$ system from the MP2/6-31G(d,p) calculations. Relative energies indicated are in kilojoules per mole and include zpve corrections.

diagram). The potential energy of this MECP is at 259 kJ mol^{-1}, while **TS(CP3→11+23)** which is the following transition structure lies at 264 kJ mol^{-1}.

An alternative reaction path, not considered explicitly in our earlier work, has now been examined:

$$^1HONH_3^+ \ (\mathbf{26}) \rightarrow {}^3O \ (\mathbf{13}) + NH_4^+ \ (\mathbf{24}) \qquad (14)$$

Although the found MECP, **CP4** at 245 kJ mol^{-1}, is approximately of the same potential energy as **CP3**—reaction 14 is severely hampered by a high-lying transition structure, **TS-(CP4→13+24)** at 326 kJ mol^{-1}. The situation is illustrated in Figure 3. This figure shows why we observe loss of NH in the experiment, but not loss of O.

Concluding Remarks

The unimolecular chemistry of hydrogen peroxide in its protonated form has been examined using quantum chemical methods. On the basis of the computational data, and in accordance with experimental and theoretical studies of analogous systems, we conclude that the most prevalent unimolecular reaction of $HOOH_2^+$ is formation of ^3O and H_3O^+ (Figure 1). By comparison with the ab initio data on H_2O_2 by Schröder et al.[41] it is evident that protonation activates hydrogen peroxide by lowering the critical energy from $E_a = 230$ kJmol^{-1} for the reaction

$$^1HOOH \rightarrow {}^3O + H_2O \qquad (15)$$

to a value of $E_a = 164$ kJ mol^{-1} for

$$^1HOOH_2^+ \rightarrow {}^3O + H_3O^+ \qquad (16)$$

It is known[34,35,42] that the triplet oxygen atom may insert relatively easily into a C−H bond of a hydrocarbon, as in

$$^3O + R{-}H \rightarrow ROH \qquad (17)$$

In addition to this, there are numerous examples,[43−45] chemical and biochemical, in the literature where the following homologous sequences of events have been recorded

$$Fe^{n+} + H_2O_2 \rightarrow FeO(H){-}OH^{n+} \qquad (18)$$

$$FeO(H){-}OH^{n+} \rightarrow FeO^{n+} + H_2O \qquad (19)$$

$$FeO^{n+} + RH \rightarrow Fe^{n+} + ROH \qquad (20)$$

The close parallel between reactions 16−17 and 18−20 is noticed, which certainly inspires us for further experimental and computational investigations.

The computational evidence presented by Bach and coworkers[12] reveals that the critical energy for oxidation of alkanes (including methane) by protonated hydrogen peroxide is negligible

$$CH_4 + HOOH_2^+ \rightarrow CH_3OH_2^+ + H_2O \qquad (21)$$

The results given in the present paper and those of Bach et al. require further experimental studies of the unimolecular and bimolecular chemistry of protonated hydrogen peroxide. Our own efforts to perform such experiments have so far been repressed by a number of practical difficulties. First, samples of concentrated hydrogen peroxide are fragile to explosion. Second, sample introduction into a high or ultrahigh vacuum chamber is difficult because H_2O_2 decomposes extremely easily into H_2O and O_2 on steel walls. Third, protonation must be soft, i.e., the difference in PA between the corresponding base of the proton donor and H_2O_2 must not be too high, to avoid direct decomposition of $HOOH_2^+$ into ^3O and H_3O^+. Recent progress in our laboratory now makes us optimistic that this interesting field soon will be available for experimental investigation.

Acknowledgment. The authors wish to thank NFR (The Norwegian Research Council) for computer time. We are also indebted to one reviewer and Professor Arne Haaland, Oslo, for suggestions regarding the O−O bond shortening problem.

References and Notes

(1) Thiel, W. R. *Angew. Chem., Int. Ed. Engl.* **1999**, *38*, 3157.
(2) Anastas, P. T.; Williamson, T. C. *Green Chemistry-Frontiers in Benign Chemical Syntheses and Processes*; Oxford University Press: Oxford, U.K., 1998.
(3) Cotton, F. A.; Wilkinson, G. *Advanced Inorganic Chemistry*; John Wiley & Sons: New York, 1988.
(4) *Cytochrome P-450. Structure, mechanism and biochemistry*; Ortiz de Montellano, G. R., Ed.; Plenum Press: New York, 1986.
(5) Que, L.; Dong, Y. *Acc. Chem.* **1996**, *29*, 190.
(6) Everse, J.; Everse, K. E.; Grisham, M. B. *Peroxidases in biology and chemistry*; CRC Press: Boca Raton, FL, 1991.
(7) Vitello, L. B.; Erman, J. E.; Miller, M. A.; Wang, J.; Kraut, J. *Biochemistry* **1993**, *32*, 9807.
(8) Loo, S.; Erman, J. E. *Biochemistry* **1975**, *14*, 3467.
(9) Toy, P. H.; Newcomb, M.; Hollenberg, P. F. *J. Am. Chem. Soc.* **1998**, *120*, 7719.
(10) Olah, G. A.; Keumi, T.; Lecoq, J. C.; Fung, A. P.; Olah, J. A. *J. Org. Chem.* **1991**, *56*, 6148.
(11) Jacquesy, J.-C.; Jouannetaud, M.-P.; Martin, A. *Bull. Soc. Fr.* **1997**, *134*, 425.
(12) Bach, R. D.; Su, M.-D. *J. Am. Chem. Soc.* **1994**, *116*, 10103.
(13) Lindinger, W.; Albritton, D. L.; Howard, C. J.; Fehsenfeld, F. C.; Ferguson, E. E. *J. Chem. Phys.* **1975**, *63*, 5220.
(14) Frisch, M. J.; Trucks, G. W.; Schlegel, H. B.; Scuseria, G. E.; Robb, M. A.; Cheeseman, J. R.; Zakrzewski, V. G.; Mongomery, J. A.; Stratmann, R. E.; Burant, J. C.; Dapprich, S.; Millam, J. M.; Daniels, A. D.; Kudin, K. N.; Strain, M. C.; Farkas, O.; Tomasi, J.; Barone, V.; Cossi, M.; Cammi, R.; Mennucci, B.; Pomelli, C.; Adamo, C.; Clifford, S.; Ochterski, J.; Petersson, G. A.; Ayala, P. Y.; Cui, Q.; Morokuma, K.; Malick, D. K.; Rabuck, A. D.; Raghavachari, K.; Foresman, J. B.; Cioslowski, J.; Ortiz, J. V.; Baboul, A. G.; Stefanov, B. B.; Liu, G.; Liashenko, A.; Piskorz, P.; Komaromi, I.; Gomperts, R.; Martin, R. L.; Fox, D. J.; Keith, T.; Al-Laham, M. A.; Peng, C. Y.; Nanayakkara, A.; Gonzalez, C.; Challacombe, M.; Gill, P. M. W.; Johnson, B. G.; Chen, W.; Wong, M. W.; Andres, J. L.; Gonzales, A.; Head-Gordon, M.; Replogle, E. S.; Pople, J. A. *GAUSSIAN 98*; Gaussian Inc.: Pittsburgh, PA, 1998.
(15) Frisch, M. J.; Pople, J. A.; Binkley, J. S. *J. Chem. Phys.* **1984**, *80*, 3265.
(16) Scott, A. P.; Radom, L. *J. Phys. Chem.* **1996**, *100*, 16502.
(17) Gonzales, C.; Schlegel, H. B. *J. Phys. Chem.* **1989**, *90*, 2154.
(18) Harvey, J. N.; Aschi, M.; Schwarz, H.; Koch, W. *Theor. Chem. Acc.* **1998**, *99*, 95.
(19) Koseki, S.; Schmidt, M. W.; Gordon, M. S. *J. Phys. Chem.* **1992**, *96*, 1347.
(20) Schmidt, M. W.; Baldridge, K. K.; Boatz, J. A.; Elbert, S. T.; Gordon, M. S.; Jensen, J. H.; Koseki, S.; Matsunaga, N.; Nguyen, K. A.; Su, S. J.; Windus, T. L.; Dupuis, M.; Montgomery, J. A. *J. Comput. Chem.* **1993**, *14*, 1347.
(21) Curtiss, L. A.; Raghavachari, K.; Pople, J. A. *J. Chem. Phys.* **1993**, *98*, 1293.
(22) Smith, B. J.; Radom, L. *Chem. Phys. Lett.* **1994**, *231*, 345.
(23) Smith, B. J.; Radom, L. *J. Am. Chem. Soc.* **1993**, *115*, 4885.
(24) Valtazanos, P.; Simandiras, E. D.; Nicolaides, C. A. *Chem. Phys. Lett.* **1989**, *156*, 240.
(25) Uggerud, E. *Mass Spectrom. Rev.* **1992**, *11*, 389.
(26) Bridgeman, A. J.; Rotherty, J. *J. Chem. Soc., Dalton Trans.* **1999**, 4077.
(27) Pearson, R. G.; Anderson, D. H.; Alt, L. L. *J. Am. Chem. Soc.* **1955**, *77*, 527.
(28) Grekov, A. P.; Veselov, V. Y. *Russ. Chem. Rev.* **1978**, *47*, 631.
(29) March, J. *Advanced Organic Chemistry-Reactions, Mechanisms, and Structure*, 3rd ed.; John Wiley & Sons: New York, 1985.
(30) Schmiedekamp, A. M.; Topol, I. A.; Michejda, C. J. *Theor. Chim. Acta* **1995**, *92*, 83.

(31) Øiestad, E. L.; Uggerud, E. *Int. J. Mass Spectrom. Ion Proc.* **1997**, *165/166*, 39.
(32) Øiestad, E. L.; Uggerud, E. *Int. J. Mass Spectrom.* **1999**, *185*−*187*, 231.
(33) Chase, M. W., Jr.; Davies, C. A.; Downey, J. R., Jr.; Frurip, D. J.; McDonald, R. A.; Syverud, A. N. *J. Phys. Chem. Ref. Data* **1985**, *14*, 1.
(34) Minaev, B. F. *Russ. J. Phys. Chem.* **1992**, *66*, 1593.
(35) Minaev, B. F.; Lunell, S. *Z. Phys. Chem.* **1993**, *182*, 263.
(36) Yarkony, D. R. *J. Phys. Chem.* **1996**, *100*, 18612.
(37) Plattner, D. A. *Angew. Chem., Int. Ed. Engl.* **1999**, *38*, 82.
(38) Poutsma, J. C.; Nash, J. J.; Paulino, J. A.; Squires, R. R. *J. Am. Chem. Soc.* **1997**, *119*, 4686.
(39) Harvey, J. N.; Aschi, M. *Phys. Chem. Chem. Phys.* **1999**, *1*, 5555.
(40) Uggerud, E. *Mass Spectrom. Rev.* **1999**, *18*, 285.
(41) Schröder, D.; Schalley, C. A.; Goldberg, N.; Hrusak, J.; Schwarz, H. *Chem. Eur. J.* **1996**, *2*, 1235.
(42) Cvetanovitc, R. J. *J. Chem. Phys. Ref. Data* **1987**, *16*, 261.
(43) MacFaul, P. A.; Arends, I. W. C. E.; Ingold, K. U.; Wayner, D. D. M. *J. Chem. Soc., Perkin Trans. 2* **1997**, 135.
(44) Schröder, D.; Schwarz, H. *Angew. Chem., Int. Ed. Engl.* **1995**, *34*, 1973.
(45) Shaik, S.; Filatov, M.; Schröder, D.; Schwarz, H. *Chem. Eur. J.* **1998**, *4*, 193.